Available online at www.sciencedirect.com
SCIENCE DIRECT®
Journal of Solid State Chemistry 177 (2004) 1359–1364
JOURNAL OF SOLID STATE CHEMISTRY
http://elsevier.com/locate/jssc

Synthesis and structures of $YNiIn_2$ and $Y_4Ni_{11}In_{20}$

Viktor Hlukhyy,[a] Vasyl' I. Zaremba,[b] Yaroslav M. Kalychak,[b] and Rainer Pöttgen[a,*]

[a] *Institut für Anorganische und Analytische Chemie, Universität Münster, Wilhelm-Klemm-Straße 8, Münster D-48149, Germany*
[b] *Inorganic Chemistry Department, Ivan Franko National University of Lviv, Kyryla and Mephodiya Street 6, Lviv 79005, Ukraine*

Received 8 October 2003; accepted 21 November 2003

Abstract

Well-shaped single crystals of $YNiIn_2$ and $Y_4Ni_{11}In_{20}$ were obtained by arc-melting of the elements and subsequent slow cooling. Both indides were investigated by X-ray diffraction on powders and single crystals: $MgCuAl_2$ type, *Cmcm*, $a = 431.52(8)$, $b = 1042.0(2)$, $c = 730.0(1)$ pm, w$R_2 = 0.0471$, 587 F^2 values, 16 variables for $YNiIn_2$ and $U_4Ni_{11}Ga_{20}$ type, *C*2/*m*, $a = 2251.2(4)$, $b = 430.77(8)$, $c = 1658.5(3)$ pm, $\beta = 124.62(1)^\circ$, w$R_2 = 0.0542$, 1583 F^2 values, 108 variables for $Y_4Ni_{11}In_{20}$. Both structures are built up from three-dimensional $[NiIn_2]$ and $[Ni_{11}In_{20}]$ networks in which the yttrium atoms fill distorted pentagonal channels. The $[NiIn_2]$ network has only Ni–In and In–In contacts, while also Ni–Ni bonding plays an important role in the $[Ni_{11}In_{20}]$ network.

Keywords: Intermetallic compounds; Crystal structure; Indium

1. Introduction

The *RE*–Ni–In systems (*RE* = rare-earth metal) have intensively been investigated in recent years [1,2] with respect to their phase relations, the crystal structures and the greatly varying magnetic and electrical properties. So far, more than 180 ternary $RE_xNi_yIn_z$ indides are known [2]. Although many of the ternary systems contain more than 10 ternary compounds, not all existing phases have yet been discovered in the isothermal sections. In many cases the structures of the unknown phases are complex. Only single-crystal data can help for such structure determinations and thus, suitable crystal growth is important.

We have recently continued our systematic phase analytical investigations in the yttrium–nickel–indium system. So far, the ternary indides YNi_9In_2 (own structure type) [3], YNi_4In ($MgCu_4Sn$ type) [4], $YNiIn_2$ ($MgCuAl_2$ type) [5], YNiIn (ZrNiAl type) [6,7], Y_2Ni_2In (Mn_2AlB_2 type) [8], $Y_2Ni_{2-x}In$ (Mo_2FeB_2 type) [9], and $Y_{12}Ni_6In$ ($Sm_{12}Ni_6In$ type) [10] have been reported. Our recent studies revealed the existence of a further ternary indide, $Y_4Ni_{11}In_{20}$, with $U_4Ni_{11}Ga_{20}$ type [11] structure. Furthermore we obtained single crystals of $YNiIn_2$. The synthesis conditions and the crystal chemistry of these two indides are reported herein.

2. Experimental

2.1. Synthesis

Starting materials for the synthesis of $YNiIn_2$ and $Y_4Ni_{11}In_{20}$ were yttrium ingots (Johnson Matthey), nickel wire (Johnson Matthey, ∅ 0.38 mm), and indium tear drops (Heraeus), all with stated purities better than 99.9%. In a first step the yttrium ingot was mechanically cut into smaller pieces and arc-melted to small buttons under an atmosphere of about 600 mbar argon in a water-cooled copper crucible [12]. The argon was purified over silica gel, molecular sieves, and titanium sponge (900 K). The pre-melting procedure strongly reduces a shattering of the elements during the strongly exothermic reaction.

The small yttrium buttons were then mixed with pieces of the nickel wire and indium tear drops in the ideal 1:1:2 and 4:11:20 atomic ratios and arc-melted as described above. Each sample was turned over and remelted three times to ensure homogeneity. The weight losses after the several melting procedures were always smaller than 0.5 wt%. After the arc-melting, $YNiIn_2$ and

*Corresponding author. Fax: +49-251-83-36002.
E-mail addresses: pottgen@uni-muenster.de, vazar@franko.lviv.ua (R. Pöttgen).

0022-4596/$ - see front matter © 2004 Elsevier Inc. All rights reserved.
doi:10.1016/j.jssc.2003.11.017

$Y_4Ni_{11}In_{20}$ were obtained only as polycrystalline powders. Special heat treatment was necessary for the growth of single crystals. Both indides were put in tantalum containers that have been sealed in evacuated silica tubes as an oxidation protection. The samples were first heated at 1270 K within 5 h and held at that temperature for 4 h. Subsequently the temperature was lowered at a rate of 5 K/h to 1020 K, then at a rate of 17.5 K/h to 670 K, and finally cooled to room temperature within 5 h. After cooling to room temperature, the samples could easily be separated from the tantalum crucibles by pounding at their base. No reaction of the samples with the crucibles could be detected. The samples are stable in air over several weeks. Single crystals exhibit metallic luster.

2.2. X-ray diffraction

The polycrystalline products have been characterized through their Guinier powder pattern. The Guinier camera was equipped with an image plate system (Fujifilm, Basread-1800) and monochromated Cu$K\alpha_1$ radiation. α-quartz ($a = 491.30$, $c = 540.46$ pm) was used as an internal standard. The orthorhombic ($YNiIn_2$) and monoclinic ($Y_4Ni_{11}In_{20}$) lattice parameters (Table 1) were obtained from least-squares fits of the powder data. The correct indexing of the patterns was ensured through intensity calculations [13] taking the atomic positions from the structure refinements. The lattice parameters determined from the powders and the single crystals agreed well. For $YNiIn_2$ we find also good agreement with the previously reported data of $a = 431.4(2)$, $b = 1040.6(5)$, and $c = 727.6(3)$ pm [5].

Small, irregularly shaped single crystals of $YNiIn_2$ and $Y_4Ni_{11}In_{20}$ were obtained by mechanical fragmentation from the annealed samples. These crystals were first examined by use of a Buerger camera equipped with an image plate system (Fujifilm BAS–1800) in order to establish suitability for intensity data collection.

Single-crystal intensity data of $YNiIn_2$ were collected at room temperature by use of a four-circle diffractometer (CAD4) with graphite monochromatized Mo$K\alpha$ (71.073 pm) radiation and a scintillation counter with pulse height discrimination. The scans were taken in the $\omega/2\theta$ mode and empirical absorption corrections were applied on the basis of psi-scan data, followed by a spherical absorption correction. The $Y_4Ni_{11}In_{20}$ intensity data were collected on a Stoe IPDS II image plate diffractometer with monochromatized Mo$K\alpha$ radiation in oscillation mode (60 mm detector distance, 20 min exposure time, ω range 0–180°, $\Delta\omega = 1°$). The integration parameters were $A = 14.5$, $B = 4.0$, and EMS = 0.014. All relevant details concerning the data collections are listed in Table 1.

Table 1
Crystal data and structure refinements for $YNiIn_2$ and $Y_4Ni_{11}In_{20}$

Empirical formula	$YNiIn_2$	$Y_4Ni_{11}In_{20}$
Molar mass (g/mol)	377.26	3297.85
Unit cell dimensions	$a = 431.52(8)$ pm	$a = 2251.2(4)$ pm
(powder data)	$b = 1042.0(2)$ pm	$b = 430.77(8)$ pm
	$c = 730.0(1)$ pm	$c = 1658.5(3)$ pm
	—	$\beta = 124.62(1)°$
	$V = 0.3282$ nm^3	$V = 1.3236$ nm^3
Space group; Z	$Cmcm$; $Z = 4$	$C2/m$; $Z = 2$
Calculated density (g/cm^3)	7.63	8.28
Crystal size (μm^3)	$20 \times 20 \times 45$	$20 \times 20 \times 150$
Transm. ratio (max/min)	1.04	2.44
Abs. coefficient (mm^{-1})	36.7	33.3
$F(000)$	660	2888
θ range for data collection	3°–40°	3°–35°
Range in $h\,k\,l$	±7, ±18, ±13	±36, ±6, ±26
Total no. of reflections	3970	4925
Independent reflections	587 ($R_{int} = 0.0500$)	1583 ($R_{int} = 0.0525$)
Reflections with $I > 2\sigma(I)$	492 ($R_{sigma} = 0.0232$)	1397 ($R_{sigma} = 0.0366$)
Data/parameters	587/16	1583/108
Goodness-of-fit on F^2	1.145	1.031
Final R indices [$I > 2\sigma(I)$]	$R_1 = 0.0235$	$R_1 = 0.0235$
	w$R_2 = 0.0446$	w$R_2 = 0.0525$
R indices (all data)	$R_1 = 0.0328$	$R_1 = 0.0290$
	w$R_2 = 0.0471$	w$R_2 = 0.0542$
Extinction coefficient	0.0090(4)	0.00033(4)
Largest diff. peak and hole	2.27 and −2.14 e/Å^3	1.08 and −1.33 e/Å^3

2.3. Structure refinements

Analysis of both diffractometer data sets revealed an orthorhombic C-centered lattice for $YNiIn_2$ and a monoclinic C-centered lattice for $Y_4Ni_{11}In_{20}$. The extinctions were compatible with space groups $Cmcm$ ($YNiIn_2$) and $C2/m$ ($Y_4Ni_{11}In_{20}$). The isotypy of $YNiIn_2$ with the $MgCuAl_2$ type [14] was readily evident from the X-ray powder data. For $Y_4Ni_{11}In_{20}$ it was not possible to distinguish between the $Ho_4Ni_{10}Ga_{21}$ [15] and the $U_4Ni_{11}Ga_{20}$ type [11] on the basis of the powder patterns.

For the first refinement cycles, the atomic parameters of $GdRhIn_2$ [16] and $Ce_4Pd_{10}In_{21}$ [17] were taken as starting values and the structures were refined using SHELXL-97 [18] (full-matrix least-squares on F^2) with anisotropic atomic displacement parameters for all atoms. The refinement for $YNiIn_2$ went smoothly to the residuals listed in Table 1 with physically meaningful displacement parameters. For $Y_4Ni_{11}In_{20}$, the equivalent isotropic displacement parameter of the In1 position was significantly larger than those of the other indium sites, indicating a much smaller scattering power on this position. Refinement of this site with the scattering power of nickel showed full occupancy. Thus, $Y_4Ni_{11}In_{20}$ adopts the $U_4Ni_{11}Ga_{20}$ type. The final cycles for $Y_4Ni_{11}In_{20}$ were then calculated with the setting of $U_4Ni_{11}Ga_{20}$ [11].

As a final check for the correct composition the occupancy parameters were refined in separate series of least-squares cycles along with the displacement parameters. All sites were fully occupied within three

Table 2
Atomic coordinates and anisotropic displacement parameters (pm^2) for $YNiIn_2$ and $Y_4Ni_{11}In_{20}$

Atom	Wyckoff position	x	y	z	U_{11}	U_{22}	U_{33}	U_{13}	U_{23}	U_{eq}
$YNiIn_2$ (space group $Cmcm$)										
Y	4*c*	0	0.06858(6)	1/4	95(2)	83(2)	99(2)	0	0	92(1)
Ni	4*c*	0	0.78756(8)	1/4	90(3)	97(3)	97(3)	0	0	94(1)
In	8*f*	0	0.35706(3)	0.04978(4)	96(1)	87(1)	79(1)	0	5(1)	88(1)
$Y_4Ni_{11}In_{20}$ (space group $C2/m$)										
Y1	4*i*	0.11911(4)	0	0.33128(5)	87(3)	88(3)	88(3)	45(2)	0	91(1)
Y2	4*i*	0.77089(4)	0	0.17413(5)	90(3)	86(3)	96(3)	53(2)	0	91(1)
Ni1	4*i*	0.0223(3)	0	0.5997(6)	136(20)	77(7)	132(10)	85(15)	0	110(8)
Ni2	4*i*	0.13619(6)	0	0.1027(1)	138(4)	88(4)	106(5)	70(4)	0	110(2)
Ni3	4*i*	0.25356(6)	0	0.61701(7)	123(4)	81(4)	98(4)	56(3)	0	104(2)
Ni4	4*i*	0.34765(6)	0	0.12117(8)	106(4)	94(4)	105(4)	58(3)	0	103(2)
Ni5	4*i*	0.50612(6)	0	0.19415(8)	107(4)	107(4)	92(4)	59(3)	0	102(2)
Ni6	2*d*	0	1/2	1/2	136(6)	101(6)	71(5)	60(5)	0	102(2)
In1	4*i*	0.0101(2)	0	0.0950(3)	105(8)	97(4)	93(4)	57(6)	0	98(3)
In2	4*i*	0.06360(3)	0	0.79047(4)	86(2)	92(2)	97(2)	49(2)	0	93(1)
In3	4*i*	0.11554(3)	0	0.55163(5)	99(2)	153(3)	117(3)	59(2)	0	124(1)
In4	4*i*	0.20217(3)	0	0.00270(4)	94(2)	77(2)	91(2)	55(2)	0	86(1)
In5	4*i*	0.24688(3)	0	0.29137(4)	99(2)	86(2)	86(2)	59(2)	0	86(1)
In6	4*i*	0.29685(3)	0	0.49757(4)	83(2)	83(2)	70(2)	35(2)	0	83(1)
In7	4*i*	0.38831(7)	0	0.3084(2)	82(6)	96(3)	107(3)	45(4)	0	100(2)
In8	4*i*	0.39834(3)	0	0.00837(4)	83(2)	81(2)	86(2)	40(2)	0	88(1)
In9	4*i*	0.54078(3)	0	0.37699(4)	88(2)	94(2)	110(2)	61(2)	0	94(1)
In10	4*i*	0.62796(7)	0	0.1955(1)	106(6)	75(3)	99(3)	63(5)	0	91(2)

U_{eq} is defined as one-third of the trace of the orthogonalized U_{ij} tensor. The anisotropic displacement factor exponent takes the form: $2\pi^2[(ha^*)^2U_{11} + \cdots + 2hka^*b^*U_{12}]$. $U_{12} = 0$.

standard deviations. The refined occupancy parameters varied between 99.9(3)% (Y) and 100.8(4)% (Ni) for $YNiIn_2$ and between 98.8(4)% (In2) and 102.8(10)% (Ni6) for $Y_4Ni_{11}In_{20}$. In the final cycles the ideal occupancy parameters were assumed again. The final difference Fourier synthesis were flat (Table 1). The positional parameters and interatomic distances of the refinements are listed in Tables 2 and 3. Listings of the observed and calculated structure factors are available.[1]

3. Results and discussion

The structures of $YNiIn_2$ and $Y_4Ni_{11}In_{20}$ have been refined from X-ray single-crystal diffractometer data. While X-ray powder data are already known for $YNiIn_2$ [5], $Y_4Ni_{11}In_{20}$ is a new compound in the ternary system Y–Ni–In. Projections along the short unit cell axis are presented in Fig. 1. All nickel atoms in $YNiIn_2$ and most of the nickel atoms in $Y_4Ni_{11}In_{20}$ have a slightly distorted trigonal prismatic coordination. These prisms are condensed via common triangular faces along the short cell periods. In the $YNiIn_2$ structure, the rows of prisms share neither corners nor edges. They are connected via Y–In and In–In bonds. This is different in the structure of $Y_4Ni_{11}In_{20}$. Here, four prisms are condensed via common edges forming a wave-like motif. Also these units are connected with each other via Y–In and In–In bonds. Between these units built up of trigonal prisms we observe a two-dimensional strand of nickel atoms surrounded by indium. This structural motif will be discussed later. The lattice parameters a of $YNiIn_2$ and b of $Y_4Ni_{11}In_{20}$ are almost similar. This is expected since almost the same geometrical motifs, i.e., nickel-centered trigonal prisms are stacked in these directions.

The Ni–In distances in both structures cover the large range from 266 to 271 pm in $YNiIn_2$ and from 259 to 310 pm in $Y_4Ni_{11}In_{20}$. The shorter of these distances compare well with the sum of the covalent radii of 265 pm [19], indicating strong covalent Ni–In bonding in these two indides. Such Ni–In distances are typically observed also in indides with different structures like $CeNiIn_2$ [20] or $LaNi_7In_6$ [21].

The structures of $YNiIn_2$ and $Y_4Ni_{11}In_{20}$ are also characterized by short In–In distances. In $YNiIn_2$ the In–In distances range from 292 to 319 pm. All of these In–In distances are shorter than in tetragonal body-centered indium [22], where each indium atom has four nearest indium neighbors at 325 pm and eight further

[1] Details may be obtained from: Fachinformationszentrum Karlsruhe, D-76344 Eggenstein-Leopoldshafen (Germany), by quoting the Registry Nos. CSD-413459 ($YNiIn_2$) and CSD-413460 ($Y_4Ni_{11}In_{20}$). mailto:crysdata@fiz-karlsruhe.de.

Table 3
Interatomic distances (pm), calculated with the lattice parameters taken from X-ray powder data of $YNiIn_2$ and $Y_4Ni_{11}In_{20}$

$YNiIn_2$											
Y:	1	Ni	292.8	Ni:	2	In	265.7	In:	1	Ni	265.7
	2	Ni	314.0		4	In	270.5		2	Ni	270.5
	4	In	316.9		1	Y	292.8		1	In	292.3
	2	In	334.3		2	Y	314.0		1	In	306.6
	4	In	341.3						2	Y	316.9
	2	Y	392.0						2	In	318.8
									1	Y	334.3
									2	Y	341.3
$Y_4Ni_{11}In_{20}$											
Y1:	2	Ni5	311.6	Ni5:	1	In8	262.4	In5:	2	Ni3	263.9
	2	In9	313.7		1	In9	266.8		1	Ni2	267.2
	2	In6	319.0		1	In10	273.0		1	In6	293.1
	2	In10	320.3		2	In1	274.2		1	In7	303.3
	1	In1	323.3		2	In2	276.1		2	In10	308.2
	2	Ni3	328.6		1	Ni4	304.7		2	Y2	314.8
	1	In5	329.8		2	Y1	311.6		1	Y1	329.8
	1	In6	332.8	Ni6:	4	Ni1	258.5		2	In3	344.2
	1	In2	340.0		2	In9	267.1	In6:	1	Ni3	265.8
	1	In3	370.1		2	In7	271.0		2	Ni3	266.2
Y2:	2	In7	314.6		4	In3	310.0		1	In5	293.1
	2	In5	314.8	In1:	2	Ni5	274.2		1	In9	300.8
	2	In4	318.1		1	Ni2	276.9		2	In6	304.8
	2	Ni4	318.2		1	In1	291.7		2	Y1	319.0
	1	In8	325.2		2	In8	298.7		2	In3	332.0
	1	In4	331.5		1	Ni2	305.3		1	Y1	332.8
	2	Ni2	334.0		2	In10	307.2	In7:	1	Ni4	269.2
	1	In2	342.7		1	In2	315.2		1	Ni6	271.0
	1	In10	343.1		1	Y1	323.3		2	Ni1	274.4
	1	In3	374.3	In2:	2	Ni4	273.0		1	In9	293.9
Ni1:	2	Ni6	258.5		1	Ni1	274.5		1	In5	303.3
	1	In3	263.5		2	Ni5	276.1		2	Y2	314.6
	1	In3	266.1		1	In4	310.6		2	In3	320.4
	2	In9	272.6		1	In1	315.2		2	In2	324.3
	2	In7	274.4		2	In9	323.4	In8:	1	Ni5	262.4
	1	In2	274.5		2	In7	324.3		2	Ni2	264.8
	1	Ni1	285.9		1	Y1	340.0		1	Ni4	268.8
Ni2:	2	In8	264.8		1	Y2	342.7		2	In1	298.7
	1	In5	267.2		2	In8	364.1		2	In4	305.3
	2	In10	271.4	In3:	1	Ni1	263.5		1	In10	308.3
	1	In1	276.9		1	Ni3	264.6		1	Y2	325.2
	1	In4	278.5		1	Ni1	266.1		2	In2	364.1
	1	In1	305.3		2	Ni6	310.0	In9:	1	Ni5	266.8
	2	Y2	334.0		2	In7	320.4		1	Ni6	267.1
Ni3:	2	In5	263.9		2	In9	321.3		2	Ni1	272.6
	1	In3	264.6		2	In6	332.0		1	In7	293.9
	1	In6	265.8		2	In5	344.2		1	In6	300.8
	2	In6	266.2		1	Y1	370.1		2	Y1	313.7
	1	In10	271.3		1	Y2	374.3		2	In3	321.3
	2	Y1	328.6	In4:	1	Ni4	269.7		2	In2	323.4
Ni4:	1	In8	268.8		2	Ni4	273.8	In10:	1	Ni3	271.3
	1	In7	269.2		1	Ni2	278.5		2	Ni2	271.4
	1	In4	269.7		2	In8	305.3		1	Ni5	273.0
	2	In2	273.0		2	In4	308.3		2	In1	307.2
	2	In4	273.8		1	In2	310.6		2	In5	308.2
	1	Ni5	304.7		2	Y2	318.1		1	In8	308.3
	2	Y2	318.2		1	Y2	331.5		2	Y1	320.3
									1	Y2	343.1

All distances within the first coordination spheres are listed. Standard deviations are all equal or less than 0.7 pm

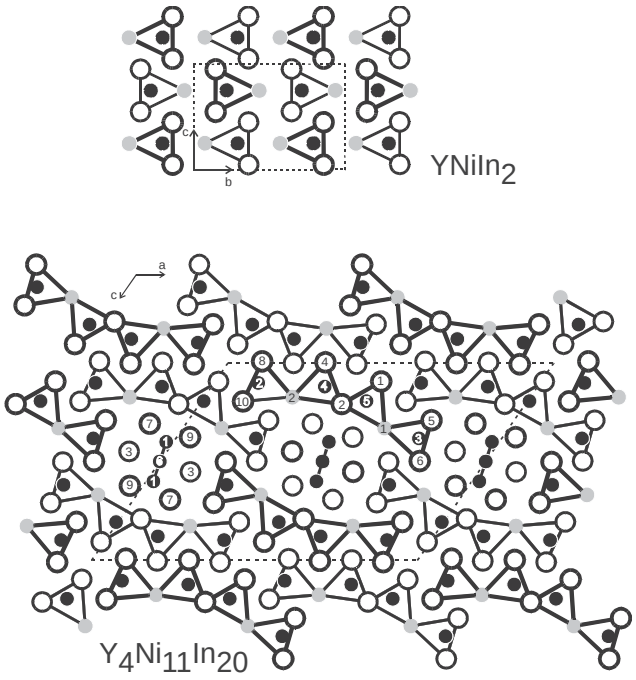

Fig. 1. Projections of the $YNiIn_2$ and $Y_4Ni_{11}In_{20}$ structures onto the *yz* and *xz* planes, respectively. All atoms lie on mirror planes at $x = 0$ (thin lines) and $x = 1/2$ (thick lines) for $YNiIn_2$, and at $y = 0$ (thin lines) and $y = 1/2$ (thick lines) for $Y_4Ni_{11}In_{20}$. The yttrium, nickel, and indium atoms are drawn as gray, filled, and open circles, respectively. The trigonal prismatic coordinations of the nickel atoms are emphasized for both structures. Atom designations are given for the $Y_4Ni_{11}In_{20}$ structure.

neighbors at 338 pm. In $Y_4Ni_{11}In_{20}$ the In–In distances cover the large range from 292 to 364 pm, but several of these distances are shorter or close to those in elemental indium. Thus, besides strong Ni–In bonding we observe also strong In–In bonding in these two structures. Together the nickel and indium atoms built complex three-dimensional $[NiIn_2]$ and $[Ni_{11}In_{20}]$ networks in which the yttrium atoms fill distorted pentagonal channels, respectively. Views of these networks are presented in Fig. 2.

The yttrium atoms in $YNiIn_2$ and $Y_4Ni_{11}In_{20}$ have coordination number 15, i.e., 3Ni + 10 In + 2Y for $YNiIn_2$, and 4Ni + 11 In atoms for both crystallographically different yttrium sites in $Y_4Ni_{11}In_{20}$. The closest Y–Y contacts in $YNiIn_2$ are at 392 pm, between the channels, while in $Y_4Ni_{11}In_{20}$ the shortest Y–Y distances at 431 pm correspond to the *b* lattice parameter. This is the direction in which the channels extend. The Y–Y distances between the channels are larger. This is a direct consequence of the yttrium content of the structures, i.e., 25 at% for $YNiIn_2$ and 11.4 at% for $Y_4Ni_{11}In_{20}$. Thus, the yttrium atoms show larger separation within the $[Ni_{11}In_{20}]$ network, although it has a similar composition to $[NiIn_2]$, i.e., $[Ni_{10}In_{20}]$.

Finally we discuss the Ni–Ni bonding in the $Y_4Ni_{11}In_{20}$ structure. As emphasized at the left-hand

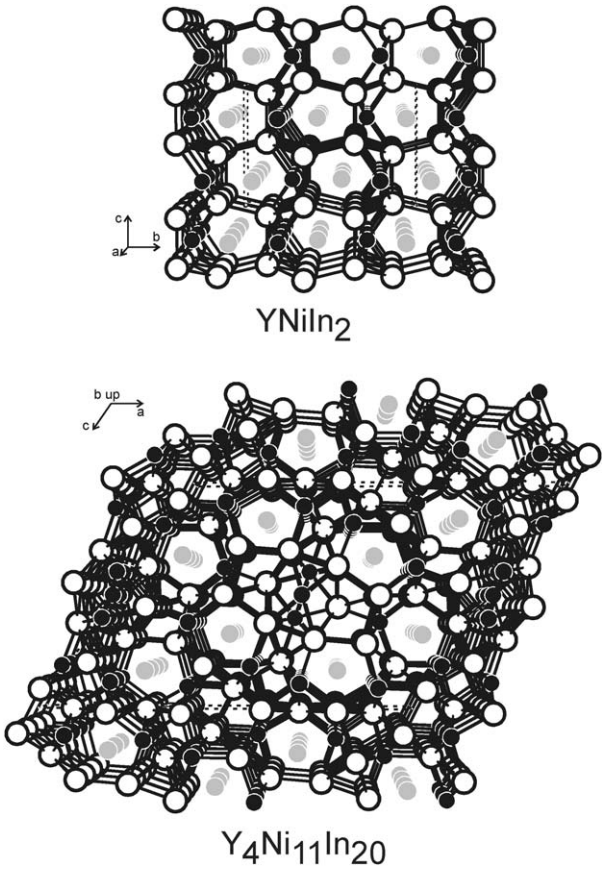

Fig. 2. Perspective views of the $YNiIn_2$ and $Y_4Ni_{11}In_{20}$ structures along the short cell axis. The yttrium, nickel, and indium atoms are drawn as gray, filled, and open circles, respectively. The three-dimensional $[NiIn_2]$ and $[Ni_{11}In_{20}]$ networks are emphasized. For details see text.

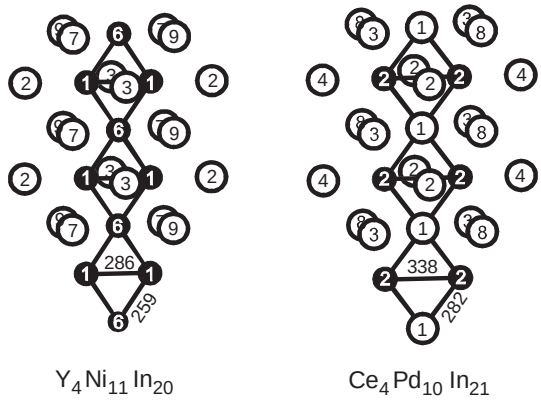

Fig. 3. Cutouts of the nickel and palladium substructures in $Y_4Ni_{11}In_{20}$ and $Ce_4Pd_{10}In_{21}$. Nickel (palladium) and indium atoms are drawn as filled and open circles, respectively. Atom designations and relevant interatomic distances are indicated.

side of Fig. 3, the Ni1 and Ni6 atoms build a two-dimensional network that is surrounded by indium atoms. The Ni–Ni distances of 259 and 286 pm, however, are slightly longer than in elemental fcc nickel (249 pm) [22]. The Ni6 position plays an important role in this peculiar structure type. Together with the four Ni1 neighbors (which have the shortest distances to Ni6), the Ni6 atoms have a slightly distorted icosahedral coordination as also discussed for $Ce_4Pd_{10}In_{21}$ [17].

If we only consider the indium neighbors of Ni6, the coordination is a slightly distorted cube. This is also a suitable coordination for indium [16,23]. Indeed, a substitution of this transition metal position by indium is realized in the series $RE_4Pd_{10}In_{21}$ (RE = La, Ce, Pr, Nd, Sm) indides [17] (Fig. 3). The structure refinements of $Y_4Ni_{11}In_{20}$ and $RE_4Pd_{10}In_{21}$ (RE = La, Ce, Pr, Nd, Sm) gave no indication for a homogeneity range, but solid solutions exist, as has recently been demonstrated for $Yb_4Ni_{10+x}Ga_{21-x}$ [24]. Thus, high-quality X-ray data are required for determination of the correct structure type, i.e., $Ho_4Ni_{10}Ga_{21}$ [15] or $U_4Ni_{11}Ga_{20}$ [11].

Acknowledgments

We are grateful to Dipl.-Ing. U.Ch. Rodewald for the intensity data collections. This work was financially supported by the Fonds der Chemischen Industrie, the Deutsche Forschungsgemeinschaft, and the Bundesministerium für Bildung, Wissenschaft, Forschung und Technologie. V.I.Z. is indebted to the Alexander von Humboldt Foundation for a research stipend.

References

[1] Ya.M. Kalychak, J. Alloys Compd. 262–263 (1997) 341.
[2] Ya.M. Kalychak, V.I. Zaremba, R. Pöttgen, M. Lukachuk, R.-D. Hoffmann, in: K.A. Gschneider Jr., V.K. Pecharsky, J.-C. Bünzli (Eds.), Handbook on the Physics and Chemistry of Rare Earths, Elsevier, Amsterdam, 2003 in press.
[3] Ya.M. Kalychak, L.G. Akselrud, V.I. Zaremba, V.M. Baranyak, Dopov. Akad. Nauk Ukr. RSR Ser. B 8 (1984) 37.
[4] V.I. Zaremba, V.M. Baranyak, Ya.M. Kalychak, Visn. Lviv Univ. Chem. 25 (1984) 18 (in Ukrainian).
[5] V.I. Zaremba, O.Ya. Zakharko, Ya.M. Kalychak, O.I. Bodak, Dopov. Akad. Nauk Ukr. RSR Ser. B 12 (1987) 44.
[6] R. Ferro, R. Marazza, G. Rambaldi, Z. Metallkd. 65 (1974) 37.
[7] Ya.M. Kalychak, V.I. Zaremba, Yu.B. Tyvanchuk, Proceedings of the Sixth International Conference on Crystal Chemistry of Intermetallic Compounds (LYIV), Abstract 77, 1995.
[8] V.I. Zaremba, V.A. Bruskov, P.Yu. Zavalij, Ya.M. Kalychak, Neorg. Mater. 24 (1988) 409 (in Russian).
[9] Ya.M. Kalychak, V.I. Zaremba, V.M. Baranyak, P.Yu. Zavalij, V.A. Bruskov, L.V. Sysa, O.V. Dmytrakh, Neorg. Mater. 26 (1990) 94 (in Russian).
[10] Ya.M. Kalychak, V.I. Zaremba, J. Stêpién-Damm, Ya.V. Galadzhun, L.G. Akselrud, Kristallografiya 43 (1998) 17 (in Russian).
[11] Yu.N. Grin, P. Rogl, J. Nucl. Mater. 137 (1986) 89.
[12] R. Pöttgen, Th. Gulden, A. Simon, GIT-Laborfachzeitschrift 43 (1999) 133.

[13] K. Yvon, W. Jeitschko, E. Parthé, J. Appl. Crystallogr. 10 (1977) 73.
[14] B. Aronsson, M. Bäckman, S. Rundqvist, Acta Chem. Scand. 14 (1960) 1001.
[15] Yu.N. Grin, Ya.P. Yarmolyuk, E.I. Gladyshevskii, Dokl. Akad. Nauk SSSR 245 (1979) 1102 (in Russian).
[16] R.-D. Hoffmann, R. Pöttgen, V.I. Zaremba, Ya.M. Kalychak, Z. Naturforsch. 55b (2000) 834.
[17] V.I. Zaremba, U.Ch. Rodewald, Ya.M. Kalychak, Ya.V. Galadzhun, D. Kaczorowski, R.-D. Hoffmann, R. Pöttgen, Z. Anorg. Allg. Chem. 629 (2003) 434.
[18] G.M. Sheldrick, SHELXL-97, Program for Crystal Structure Refinement, University of Göttingen, 1997.
[19] J. Emsley, The Elements, Oxford University Press, Oxford, 1999.
[20] V.I. Zaremba, Ya.M. Kalychak, Yu.B. Tyvanchuk, R.-D. Hoffmann, M.H. Möller, R. Pöttgen, Z. Naturforsch. 57b (2002) 791.
[21] Ya.M. Kalychak, V.I. Zaremba, Ya.V. Galadzhun, Kh.Yu. Miliyanchuk, R.-D. Hoffmann, R. Pöttgen, Chem. Eur. J. 7 (2001) 5343.
[22] J. Donohue, The Structures of the Elements, Wiley, New York, 1974.
[23] R.-D. Hoffmann, R. Pöttgen, Chem. Eur. J. 6 (2000) 600.
[24] L. Vasylechko, W. Schnelle, U. Burkhardt, R. Ramlau, R. Niewa, H. Borrmann, K. Hiebl, Z. Hu, Yu. Grin, J. Alloys Compd. 350 (2003) 9.